



*Supplement of*

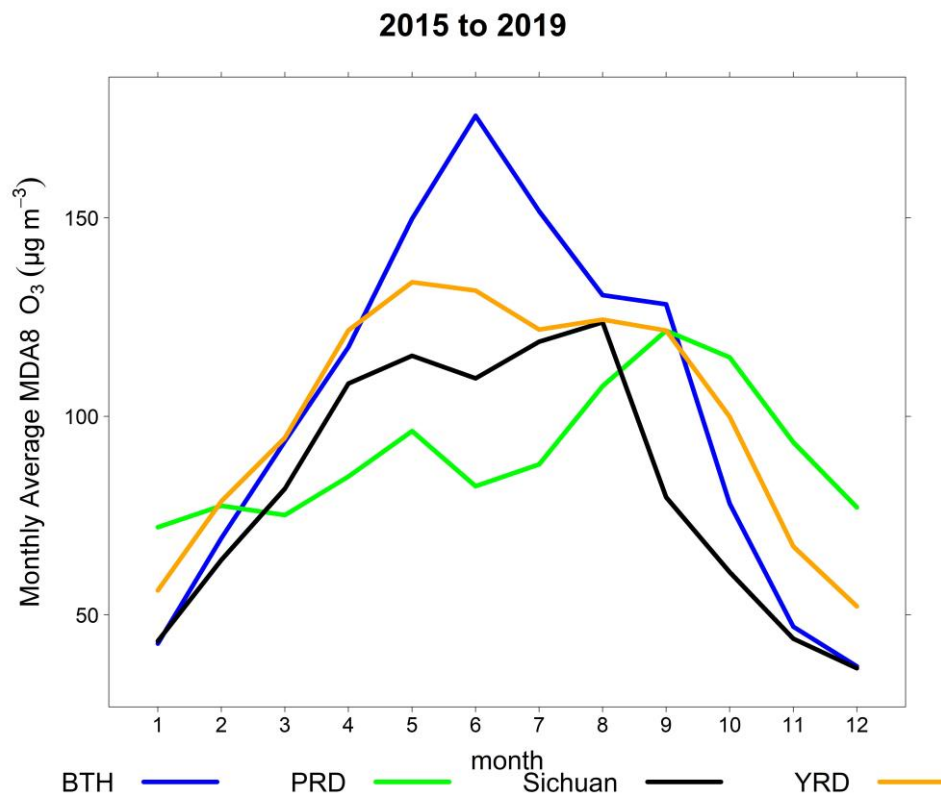
## **A machine learning approach to quantify meteorological drivers of ozone pollution in China from 2015 to 2019**

**Xiang Weng et al.**

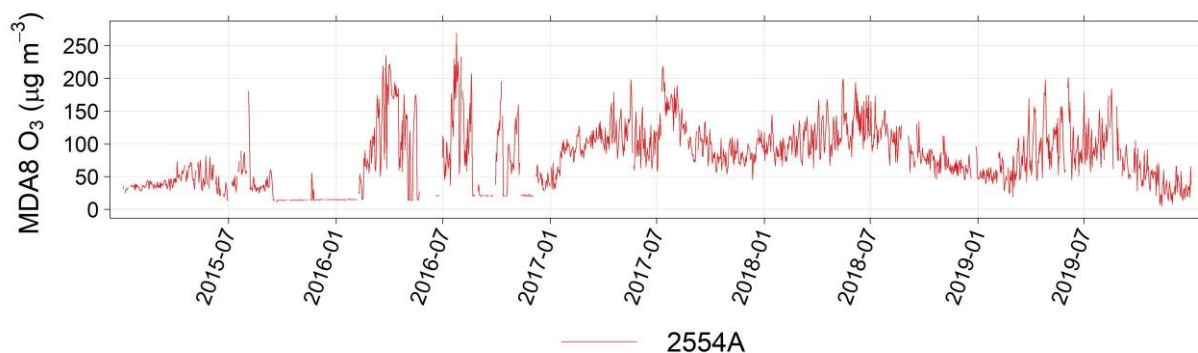
*Correspondence to:* Xiang Weng (x.weng@uea.ac.uk)

The copyright of individual parts of the supplement might differ from the article licence.

Supplementary Figures

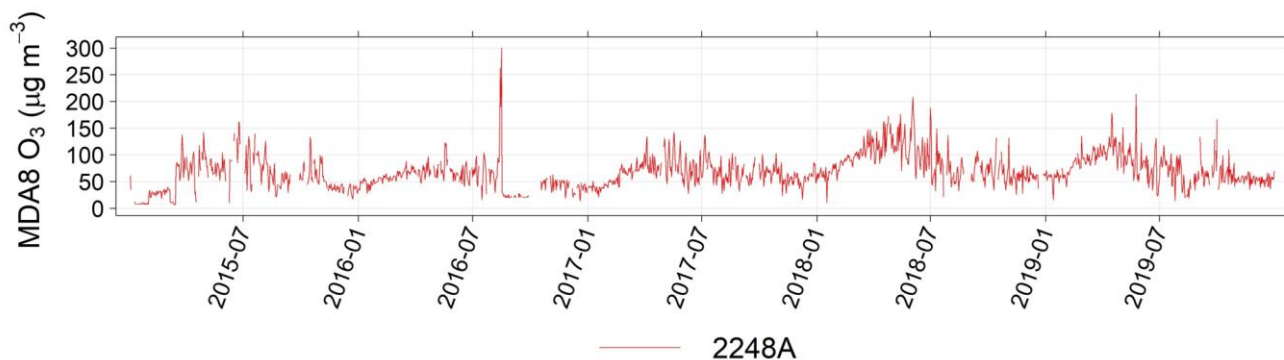


5 **Figure S1. Monthly average MDA8 ozone during 2015-2019 in 4 megacity clusters (BTH, PRD, Sichuan and YRD) of China. BTH shows a highest monthly average MDA8 ozone in June, while PRD's ozone is relatively low in summer but high in September.**



10 **Figure S2.** An example of a station's MDA8 ozone data (station ID: 2554A) that is considered to be unreliable. It is characterized by a relative long period (2015-Sep-15 to 2015-Nov-11) with MDA8 ozone consistently at  $14 \mu\text{g m}^{-3}$ . Stations in this case are not used in this study.

(a)



(b)

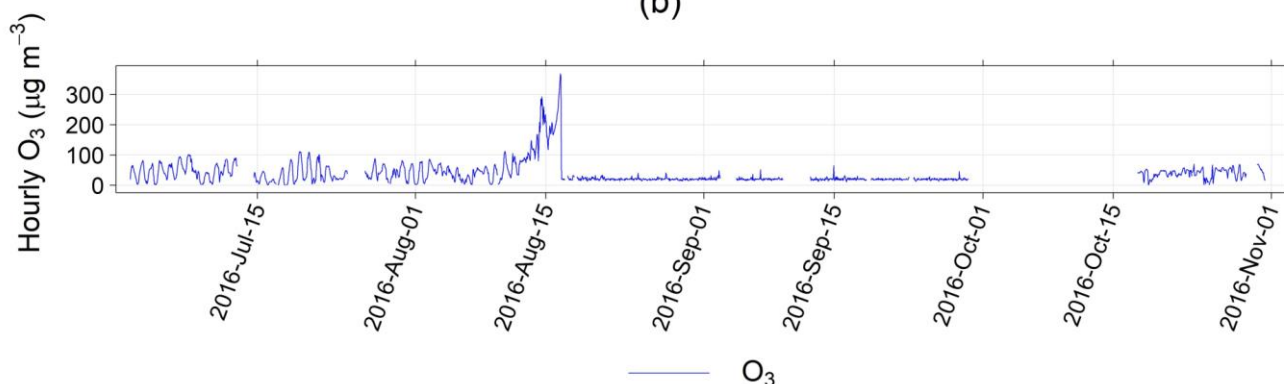


**Figure S3.** An example of a station's ozone data (station ID: 2248A) that is considered to be unreliable. A spike of MDA8 ozone (a) and hourly ozone (b) occurred on 2016-Aug-16 with at about  $300 \mu\text{g m}^{-3}$ . After the spike, hourly ozone dropped to nearly 10 to  $20 \mu\text{g m}^{-3}$  and the value remains stable throughout September and October of 2016.

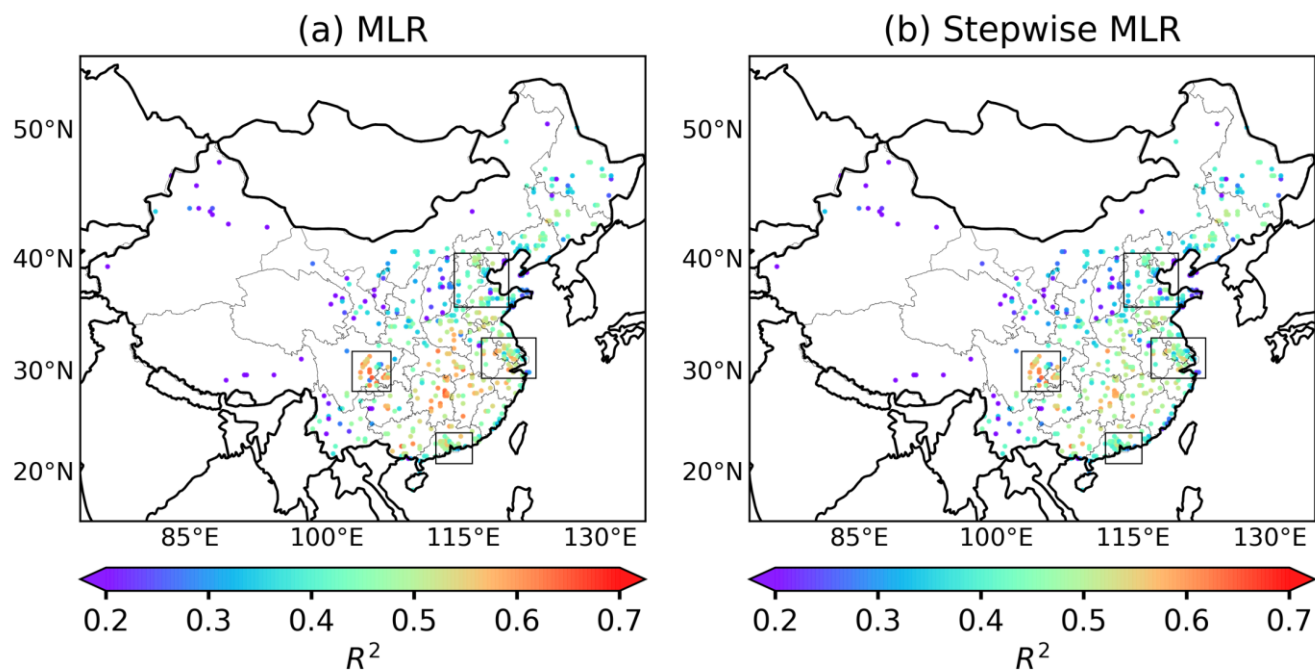


Figure S4. Coefficient of determination ( $R^2$ ) between deseasonalized observation ozone and deseasonalized predicted values of MDA8 in multiple linear regression (MLR) with all 11 meteorological predictors (a) and stepwise MLR with 3 most dominant local meteorological predictors as input (b).

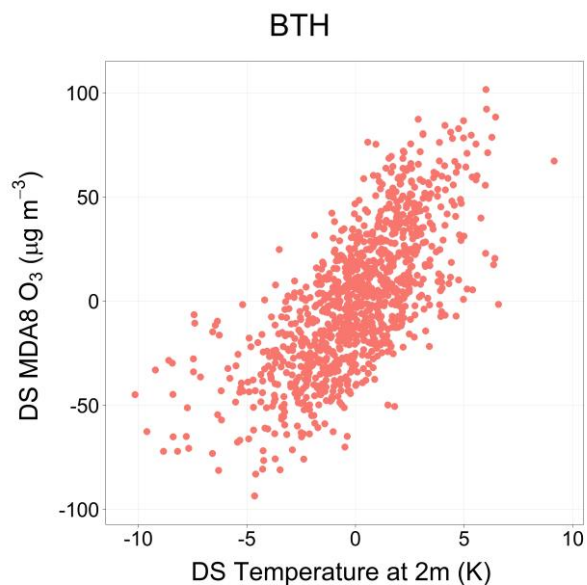
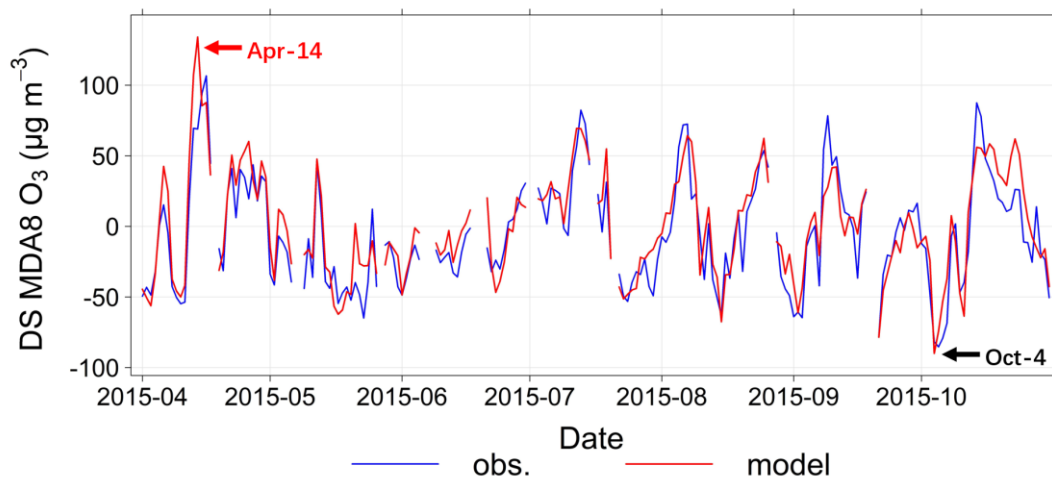
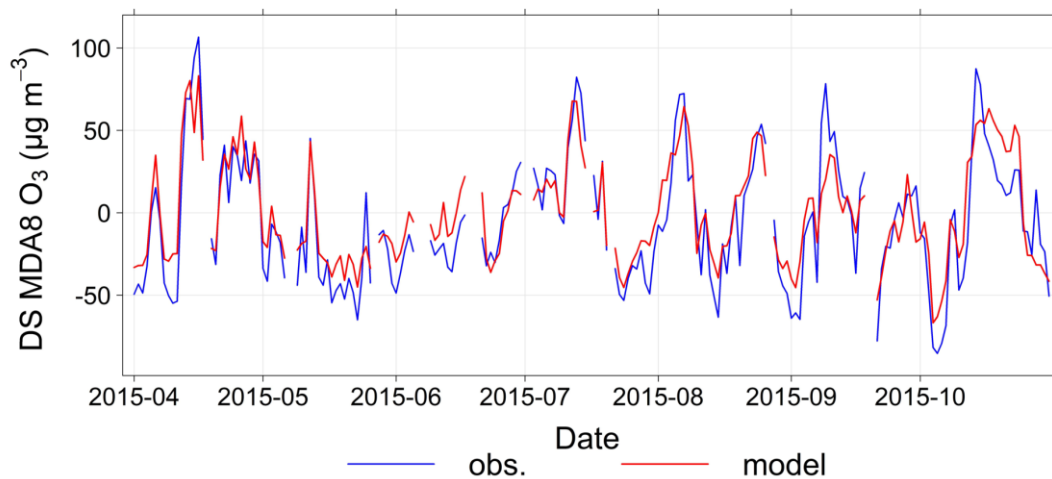


Figure S5. relationship between deseasonalized temperature at 2m and deseasonalized MDA8 ozone from April to October during 2015 to 2019 in BTH.

(a) RR-2D PRD

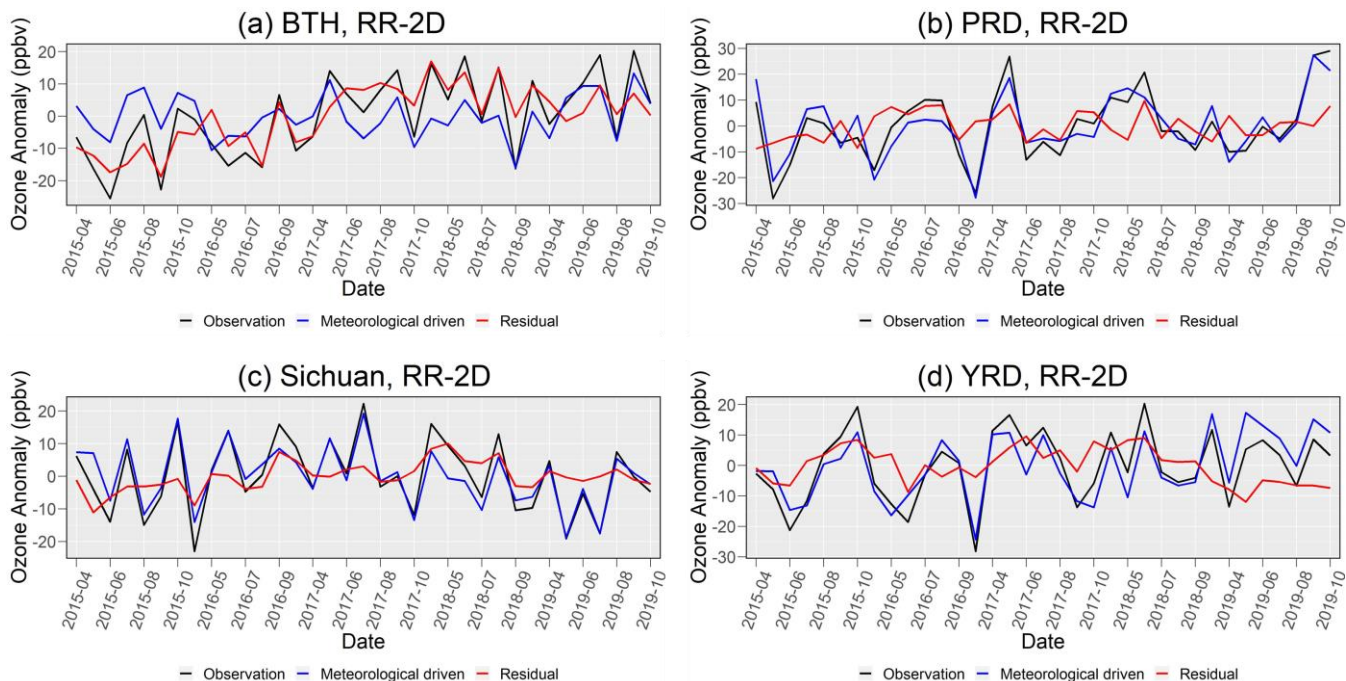


(b) RFR-2D PRD



25

Figure S6. Examples of deseasonalized ozone predicted by RR-2D (a) and RFR-2D (b) in comparison with deseasonalized observations in PRD during April to October of 2015. For the low anomaly on 2015-Oct-4 (indicated by the black arrow in the figure), RR-2D has a better prediction compared to RFR-2D, which suggests its ability of extrapolation; while the overprediction of high anomaly by RR-2D on 2015-Apr-14 (red arrow) indicates its trade-off for having a risk of over-extrapolation.



30

**Figure S7.** Time series of MDA8 ozone anomaly (ppbv) from 2015 to 2019 during April to October in BTH (a), PRD (b), Sichuan (c) and YRD (d). Monthly average ozone for each region is first calculated. Anomalies are calculated by subtracting each monthly average ozone by the corresponding month's average throughout 2015 to 2019. The black lines represent observational anomalies. The blue lines are the anomalies predicted by ridge regression–2D (RR–2D), which indicate the trends of meteorologically driven ozone anomalies. The red lines are observational ozone anomalies subtracted by meteorologically driven ozone anomalies.

35

### Supplementary Table

**Table S1.** List of stations that are not used in this study.

Station ID	Longitude	Latitude	Station ID	Longitude	Latitude
2702A	79.9117	37.1013	2288A	117.7442	30.8811
2701A	79.9485	37.1152	2287A	117.7806	30.9414
2697A	76.1861	39.7153	2286A	117.8078	30.9222
2696A	80.2956	41.1933	2285A	117.8178	30.9414
2695A	80.2828	41.1636	2271A	117.3605	32.9427
2694A	82.0806	44.8969	2260A	131.0032	45.7677
2691A	87.2997	44.0114	2248A	131.1638	46.6572
2679A	106.196	37.9723	2223A	120.3939	41.615
2678A	106.2025	37.9844	2181A	112.7383	38.4519

2677A	106.1532	37.9648	2175A	110.9956	35.0147
2676A	97.3731	37.3753	2174A	112.7105	37.7087
2674A	100.2561	34.4714	2173A	112.7306	37.7111
2655A	100.4497	38.9389	2168A	112.4254	39.3179
2654A	100.4686	38.9467	2167A	112.4549	39.3606
2648A	104.1731	36.5481	2166A	112.44	39.3514
2630A	80.1161	32.5	2161A	112.835	35.4934
2624A	91.7608	29.2313	2054A	114.1044	32.1078
2618A	98.8601	25.8567	2010A	119.7183	30.2366
2604A	100.0782	23.8982	1998A	119.18	31.955
2601A	100.98	22.7633	1997A	119.146	31.955
2599A	100.2497	26.8802	1983A	121.531	36.913
2590A	104.8811	25.0992	1981A	122.038	37.197
2580A	104.9544	26.5506	1958A	86.2381	41.7128
2556A	103.0001	29.9816	1957A	86.2022	41.7192
2555A	103.0109	29.9834	1953A	85.1186	45.6886
2554A	103.0013	29.9899	1952A	84.8897	45.5828
2521A	107.3476	22.4137	1951A	84.8861	45.6033
2520A	109.2317	23.7369	1945A	98.2908	39.7711
2518A	108.1009	24.6967	1943A	102.1725	38.5339
2515A	111.5622	24.4072	1801A	118.48	31.6928
2498A	111.26	23.4794	1796A	118.3667	31.3139
2497A	111.2353	23.415	1795A	118.37	31.4189
2496A	111.3178	23.475	1794A	118.3528	31.3508
2495A	111.2897	23.4792	1780A	123.9305	47.3386
2491A	111.9892	27.7044	1369A	113.628	22.4251
2409A	115.6558	34.429	1362A	113.891	22.5794
2405A	112.5003	32.9735	1279A	117.124	31.8516
2400A	114.005	33.568	1278A	117.278	31.7386
2374A	114.3703	27.7914	1277A	117.302	31.7956
2369A	114.99	27.1311	1276A	117.336	31.8585
2318A	118.7175	30.9431	1275A	117.266	31.9438
2317A	118.7386	30.9742	1274A	117.25	31.8572
2316A	118.7581	30.9447	1269A	119.879	28.4231
2311A	115.8067	33.8399	1164A	120.613	31.2703
2310A	116.5661	31.7712	1103A	123.428	41.8472
2308A	116.478	31.7618	1090A	111.651	40.7579
2307A	116.508	31.7371	1084A	112.469	37.7124
2306A	116.989	33.6306			

2303A	115.8556	32.8603
2299A	118.3244	32.2786
2298A	118.3094	32.3153
2297A	118.1371	30.2756
2296A	118.3236	29.7207
2295A	118.3057	29.7128
2294A	116.9896	30.6145
2292A	117.0331	30.512
2291A	117.0549	30.5103
2290A	117.8472	30.9697
2289A	117.8561	30.9219